

Adenophostin-mediated quantal Ca^{2+} release in the purified and reconstituted inositol 1,4,5-trisphosphate receptor type 1

Junji Hirota^{a,b,*}, Takayuki Michikawa^a, Atsushi Miyawaki^a, Masaaki Takahashi^c,
Kazuhiko Tanzawa^c, Ichiro Okura^b, Teiichi Furuichi^a, Katsuhiko Mikoshiba^{a,d}

^aDepartment of Molecular Neurobiology, Institute of Medical Science, University of Tokyo, 4-6-1 Shirokanedai, Minato-ku, Tokyo 108, Japan

^bDepartment of Bioengineering, Tokyo Institute of Technology, 4259 Nagatsuta, Midori-ku, Yokohama 226, Japan

^cThe Biological Research Laboratories, Sankyo Co. Ltd., 1-2-58 Hiromachi, Shinagawa-ku, Tokyo 140, Japan

^dMolecular Neurobiology Laboratory, The Institute of Physical and Chemical Research (RIKEN), Tsukuba Life Science Center, 3-1-1 Koyadai, Tsukuba-shi, Ibaragi 305, Japan

Received 2 May 1995; revised version received 29 May 1995

Abstract Kinetics of Ca^{2+} release by adenophostin, a novel agonist of inositol 1,4,5-trisphosphate (IP_3) receptor, in the purified and reconstituted IP_3 receptor type 1 ($\text{IP}_3\text{R1}$) was investigated using the fluorescent Ca^{2+} indicator fluo-3. Submaximal concentrations of adenophostin caused quantal Ca^{2+} release from the purified $\text{IP}_3\text{R1}$ as IP_3 did. Adenophostin-induced Ca^{2+} release by the purified $\text{IP}_3\text{R1}$ exhibited a high positive cooperativity ($nH = 3.9 \pm 0.2$, $\text{EC}_{50} = 11 \text{ nM}$), whereas the IP_3 -induced Ca^{2+} release exhibited a moderate one ($nH = 1.8 \pm 0.1$, $\text{EC}_{50} = 100 \text{ nM}$). Inhibition of [^3H] IP_3 binding to the purified $\text{IP}_3\text{R1}$ by adenophostin exhibited a positive cooperativity ($nH = 1.9$, $K_i = 10 \text{ nM}$), whereas IP_3 did not ($nH = 1.1$, $K_i = 41 \text{ nM}$).

Key words: Inositol 1,4,5-trisphosphate;
Inositol 1,4,5-trisphosphate receptor; Quantal Ca^{2+} release;
Adenophostin

1. Introduction

Inositol 1,4,5-trisphosphate (IP_3), a second messenger derived from the hydrolysis of phosphatidylinositol 4,5-bisphosphate, is responsible for Ca^{2+} release from intracellular calcium stores [1]. IP_3 receptor (IP_3R) is an IP_3 -activated Ca^{2+} release channel and plays a crucial role in Ca^{2+} signaling in a variety of cell functions. Thus, kinetic studies of IP_3 -induced Ca^{2+} release (IICR) are fundamental for elucidating the mechanisms underlying intracellular dynamics of Ca^{2+} signaling. Recent molecular cloning studies have revealed that there are at least three types of the IP_3R from distinct genes [2–4]. Differences in the primary sequences, especially in the modulator domains including putative phosphorylation and modulator-binding sites, among these IP_3R types suggest that there may be differences in Ca^{2+} release properties of each receptor type [5]. It is now known that these different IP_3R types often coexist in single cells [6]. Therefore, to study the kinetics of IICR, each IP_3R type should be investigated independently. This would allow us to relate differences in the structure of each IP_3R type to differences in the Ca^{2+} release kinetics.

*Corresponding author. Fax: (81) (3) 5449-5420.

Abbreviations: IP_3 , D-myo-inositol 1,4,5-trisphosphate; IP_3R , IP_3 receptor; $\text{IP}_3\text{R1}$, IP_3R type 1; CHAPS, 3-[(3-cholamidopropyl)dimethylammonio]-1-propanesulfonic acid; HEPES, N-(2-hydroxyethyl)piperazine-N'-2-ethanesulfonic acid.

To understand the mechanisms and roles of IICR underlying intracellular Ca^{2+} signalling, development of specific agonists and antagonists with high affinity for IP_3R are needed. There are few pharmacological reagents available for analysis of IICR. No specific antagonist for IICR is known, but heparin inhibits IP_3 binding to the IP_3R in a non-specific manner. On the other hand, novel agonists, adenophostin A and B, have been isolated recently as fungal products [7]. Adenophostin is the most potent agonist, which has higher binding affinity and Ca^{2+} release activity than the native ligand, IP_3 .

Recently, we have investigated the kinetics of IP_3R type 1 ($\text{IP}_3\text{R1}$)-mediated IICR using the fluorescent Ca^{2+} indicator fluo-3, and reported that the $\text{IP}_3\text{R1}$ -mediated IICR exhibited a positive cooperativity ($nH = 1.8$), quantal Ca^{2+} release and biphasic nature (Hirota et al., submitted). In the present study, to define the properties of the new agonist adenophostin, we have investigated the kinetics of Ca^{2+} release induced by adenophostin (adenophostin B) and compared the kinetics with that by IP_3 in terms of the cooperativity, quantal and biphasic nature of $\text{IP}_3\text{R1}$ -mediated Ca^{2+} release.

2. Materials and methods

2.1. Materials

IP_3 , fluo-3 and CHAPS were obtained from Dojindo Laboratories (Kumamoto, Japan), Chelex-100 from Bio-Rad, DTPA-conjugated polymetal-sponge from Molecular Probes, phosphatidylcholine, phosphatidylserine and cholesterol from Avanti Polar-Lipids, INC. All other reagents used were of analytical grade or the highest grade available. Adenophostin (adenophostin B) was isolated from the culture broth of *Penicillium Brevicompactum* SANK11991 [8].

2.2. Purification of IP_3R type 1 ($\text{IP}_3\text{R1}$)

$\text{IP}_3\text{R1}$ was purified type-specifically from mouse cerebellar microsomal fraction by using an immunoaffinity column conjugated with an anti-pep 6 antibody, a polyclonal antibody against $\text{IP}_3\text{R1}$ C-terminus, as reported previously [9].

2.3. Reconstitution of the purified $\text{IP}_3\text{R1}$

The purified $\text{IP}_3\text{R1}$ was reconstituted into lipid vesicles by the dialysis method. Phosphatidylcholine, phosphatidylserine and cholesterol dissolved in chloroform were mixed to give a concentration of 3, 1 and 0.8 mg/ml, respectively. The lipid mixture was dried to a thin film under a stream of nitrogen gas and then under vacuum. The lipid film was suspended at 2 mg/ml in buffer A (100 mM KCl, 1 mM 2-mercaptoethanol, 10 mM HEPES-KOH (pH 7.4) and 4 mM CaCl_2) containing 1% CHAPS. The immunoaffinity purified $\text{IP}_3\text{R1}$ was concentrated by using Centrprep 100 (Amicon) to give a protein concentration of 100 $\mu\text{g/ml}$. The concentrated $\text{IP}_3\text{R1}$ solution was mixed with buffer A containing lipids and detergent to give final $\text{IP}_3\text{R1}$, lipids and CHAPS of 50 $\mu\text{g/ml}$, 0.5 mg/ml and 1%, respectively. After 20 min incubation on ice with

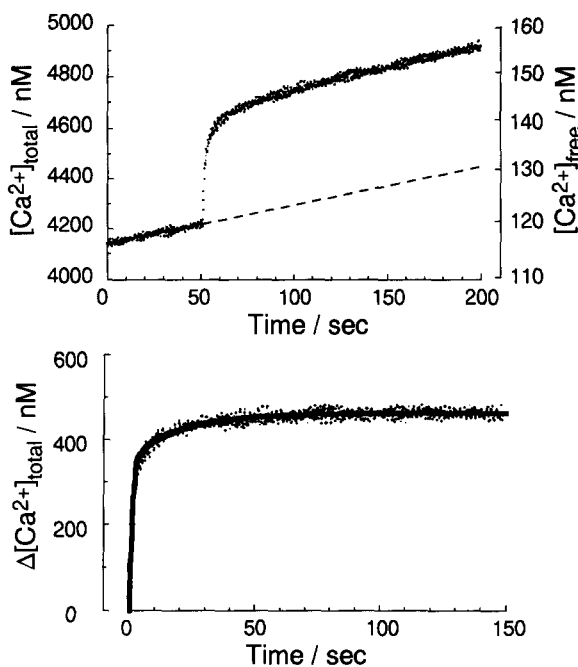


Fig. 1. Typical profile of Ca^{2+} release by adenophostin in the purified and reconstituted IP_3R1 . Changes of fluorescence of the Ca^{2+} indicator fluo-3 were recorded after injection of 15 nM adenophostin. Adenophostin-induced Ca^{2+} release from the liposomes was followed by a constant leakage of Ca^{2+} (the dotted line). (B) The net Ca^{2+} release was obtained by extrapolating and subtracting the constant Ca^{2+} leakage from the profile. The profile of net Ca^{2+} release was found to be well fitted by a biexponential (the solid line) with the fast and slow rate constants.

occasional gentle stirring, the IP_3R1 -lipid mixtures were dialyzed for 72 hours against 8 changes of a 500-fold volume excess of buffer A at 4°C. The resulting proteoliposomes (IP_3R1 in lipid vesicles) were pelleted by centrifugation at $100,000 \times g$ for 30 min at 2°C, and were washed with buffer B (buffer A with 10 μM fluo-3 but no Ca^{2+}) twice, and were resuspended with buffer B to the same volume used before dialysis. After incubation for 10 min at 25°C, the resuspended proteoliposomes were passed over Chelex-100 to remove extravesicular Ca^{2+} , and then were used for Ca^{2+} release assay.

2.4. Measurements of adenophostin- and IP_3 -induced Ca^{2+} release

Adenophostin- and IP_3 -induced Ca^{2+} efflux from the proteoliposomes were measured by monitoring the fluorescence changes of fluo-3. Briefly, fluorometric measurements of Ca^{2+} release were performed by using an F-2000 fluorometer (Hitachi Inc.). The excitation and emission wavelengths were 500 and 525 nm, respectively, with 10 nm bandpass. Measurements were made at 25°C in a 0.5×0.5 cm quartz cuvette containing 0.4 ml of the proteoliposome solution with continuous-stirring by a Teflon stir bar. Ca^{2+} release was monitored after addition of 2 μl adenophostin or IP_3 to give the desired concentrations. The data was acquired every 200 ms. The fluorescent intensities of fluo-3 were calibrated to free Ca^{2+} concentrations using a Ca^{2+} calibration kit with modification of pH to 7.4 (Molecular Probes). The calibration curve gave the dissociation constant of fluo-3 for Ca^{2+} of 170 nM, which was used to estimate the free and total Ca^{2+} concentrations. To exclude the possibility of feedback regulation by the released Ca^{2+} , we used 10 μM fluo-3, which was high enough to chelate the released Ca^{2+} and to keep deviations of extravesicular free Ca^{2+} concentration within 10–30 nM. Extravesicular free Ca^{2+} concentrations prior to addition of adenophostin or IP_3 were approximately 100 nM throughout the experiments.

2.5. [3H] IP_3 binding assay

[3H] IP_3 binding assay was performed by the polyethylene glycol precipitation method [10]. 0.5 μg of the purified IP_3R1 was incubated in

50 μl of the solution containing 50 mM Tris-HCl, pH 8.0, 1 mM EDTA, 1 mM 2-mercaptoethanol, 9.6 nM [3H] IP_3 , and either adenophostin or cold IP_3 , for 10 min at 4°C. Non-specific binding was measured in the presence of 100 nM adenophostin or 2 μM IP_3 .

3. Results and discussion

3.1. Measurement of Ca^{2+} release induced by adenophostin and IP_3

In this study, we have investigated the kinetics of adenophostin- and IP_3 -induced Ca^{2+} release by a single member of the IP_3R family in artificial membrane vesicles, thereby excluding the possibilities of modulation of Ca^{2+} release kinetics by factors such as IP_3 metabolism, Ca^{2+} pumping activity, involvement of molecules sensing changes in Ca^{2+} concentration and heterogeneity of IP_3R types. As we used high enough concentration of fluo-3 to keep extravesicular free Ca^{2+} concentration almost constant as described in section 2, we could expect to rule out the possibility of the feedback regulation of the subsequent Ca^{2+} release activity by changes of extravesicular free Ca^{2+} concentrations, which have been observed in permeabilized cell systems [11,12] and microsomal assays [13,14].

Fig. 1 shows a typical profile of adenophostin-induced Ca^{2+} release by the immunoaffinity-purified IP_3R1 reconstituted into lipid vesicles. 15 nM adenophostin-induced Ca^{2+} release from the liposomes followed a constant leakage of Ca^{2+} (Fig. 1A), which was linear over the time range of the measurements, confirming that adenophostin is a true agonist of IP_3R1 . The net Ca^{2+} release (Fig. 1B) was obtained by extrapolating and subtracting the constant Ca^{2+} leakage (Fig. 1A) from the profile. The net IICR could not be fitted by a single exponential but was found to be a biexponential (Fig. 1B) with the fast

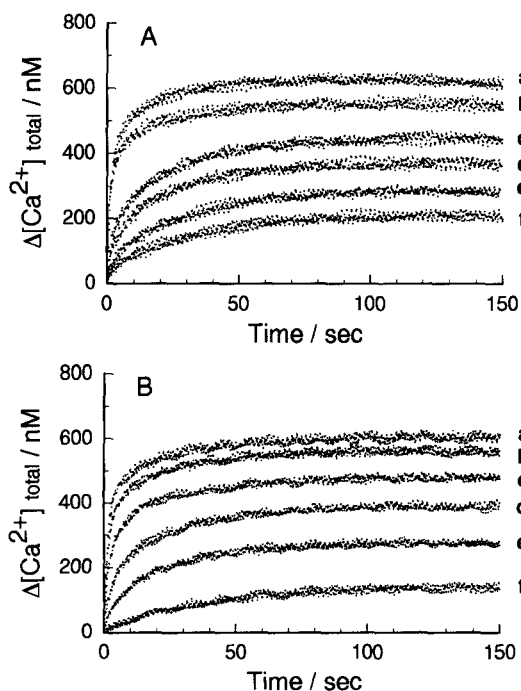


Fig. 2. Time course of Ca^{2+} release following the injection of different concentrations of agonist. Adenophostin- and IP_3 -induced Ca^{2+} release at different concentrations of IP_3 were performed on a single batch of proteoliposomes. (A) [adenophostin] = 100 nM (a), 50 nM (b), 11 nM (c), 9 nM (d), 7 nM (e), 5 nM (f). (B) [IP_3] = 5 μM (a), 500 nM (b), 200 nM (c), 70 nM (d), 40 nM (e) and 20 nM (f).

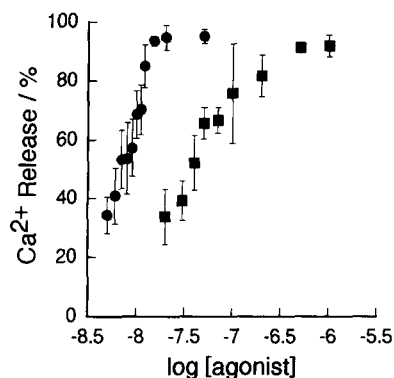


Fig. 3. The amounts of released Ca^{2+} plotted as a function of concentrations of adenophostin (●) and IP_3 (■). The amounts of released Ca^{2+} were plotted as a function of adenophostin and IP_3 concentrations. The data were normalized to the amplitude for 100 nM adenophostin and 5.0 μM IP_3 (values are mean \pm S.D., $n = 3-4$).

and slow rate constants ($k_{\text{fast}} = 0.63 \pm 0.02 \text{ s}^{-1}$ ($76 \pm 1\%$), $k_{\text{slow}} = 0.050 \pm 0.002 \text{ s}^{-1}$ ($24 \pm 1\%$)), indicating that in response to adenophostin the purified $\text{IP}_3\text{R1}$ has two states to release Ca^{2+} .

$$\Delta[\text{Ca}^{2+}]_{\text{total}} = T(1 - A_{\text{fast}} \cdot e^{-k_{\text{fast}} \cdot t} - A_{\text{slow}} \cdot e^{-k_{\text{slow}} \cdot t}) \quad (1)$$

where T represents a total amount of released Ca^{2+} , A is amplitude of the fast and slow components (%) ($A_{\text{fast}} + A_{\text{slow}} = 100\%$), k is rate constant (s^{-1}) and t is time (s).

3.2. Kinetics of adenophostin- and IP_3 -induced Ca^{2+} release

Different concentrations of adenophostin and IP_3 were added to obtain dose-response curves. Fig. 2A and B show typical time courses of Ca^{2+} release by adenophostin and IP_3 , respectively, from the same batch of proteoliposomes. These profiles were found to be biexponential. Submaximal concentrations of adenophostin and IP_3 caused partial Ca^{2+} release, and rates of Ca^{2+} release were dependent on the adenophostin and IP_3 concentrations. After full Ca^{2+} release by maximal concentrations of adenophostin and IP_3 , no additional Ca^{2+} release was evoked by additions of IP_3 and adenophostin, respectively (data not shown). The amounts of released Ca^{2+} by maximal doses of adenophostin and IP_3 were identical.

Relative amounts of released Ca^{2+} at various concentrations of adenophostin and IP_3 are shown in Fig. 3 ($n = 3-4$). The amount of released Ca^{2+} increased as a function of adenophostin and IP_3 concentrations, indicating that adenophostin is capable of producing the quantal response of Ca^{2+} release by the purified $\text{IP}_3\text{R1}$ as IP_3 did. These results suggest that the quantal Ca^{2+} release is not a unique phenomenon to the native ligand, IP_3 , but is an intrinsic property of $\text{IP}_3\text{R1}$.

The initial rates of Ca^{2+} release varied with adenophostin and IP_3 concentrations and saturated above 20 nM adenophostin and 1 μM IP_3 (Fig. 4A). Half-maximal initial rates of Ca^{2+} release occurred at 11 nM adenophostin and 100 nM IP_3 , indicating that adenophostin was approximately 10-fold more potent than the native ligand, IP_3 , in Ca^{2+} releasing activity. However, in the previous experiments using rat cerebellar microsomes, adenophostin was 100-fold more potent than IP_3 [7]. The difference in the potencies of Ca^{2+} releasing activity obtained may be due to different assay systems used.

3.3. Cooperativity of ligand binding and Ca^{2+} releasing activity of $\text{IP}_3\text{R1}$ by adenophostin and IP_3

The extent of cooperativity of Ca^{2+} release is an important and fundamental issue for understanding the channel opening mechanism. In previous reports, there is controversy about the cooperativity of IICR, i.e. no cooperativity [13,14] or positive cooperativity ($n_H = 2$) [15,16] ($n_H = 4$) [17] has been reported. We determined the degree of cooperativity of $\text{IP}_3\text{R1}$ -mediated Ca^{2+} release by Hill plotting using initial rates of Ca^{2+} release (Fig. 4B). The slopes in the Hill plots over the range of submaximal concentrations of adenophostin (5–15 nM) and IP_3 (20–200 nM) were 3.9 ± 0.2 and 1.8 ± 0.1 , respectively, indicating that adenophostin-induced Ca^{2+} release by the purified $\text{IP}_3\text{R1}$ exhibited a high positive cooperativity ($n_H = 3.9 \pm 0.2$), whereas the IP_3 -induced Ca^{2+} release exhibited a moderate one ($n_H = 1.8 \pm 0.1$). The results suggest that at least four molecules of adenophostin or two molecules of IP_3 per one $\text{IP}_3\text{R1}$ -channel are needed for Ca^{2+} release.

As both adenophostin- and IP_3 -induced Ca^{2+} release consist of two sequential events, i.e. ligand-binding and channel opening, we have studied the cooperativity of ligand binding to the purified $\text{IP}_3\text{R1}$. Fig. 5 shows inhibition curves of [^3H] IP_3 binding to the purified $\text{IP}_3\text{R1}$ by various concentrations of adenophostin and IP_3 . Adenophostin inhibited [^3H] IP_3 binding to the purified $\text{IP}_3\text{R1}$ with higher potency ($\text{IC}_{50} = 19 \text{ nM}$) than IP_3 ($\text{IC}_{50} = 76 \text{ nM}$). The apparent inhibition constants (K_i) for adenophostin and IP_3 were calculated to be 10 nM and 41 nM, respectively, using following equation.

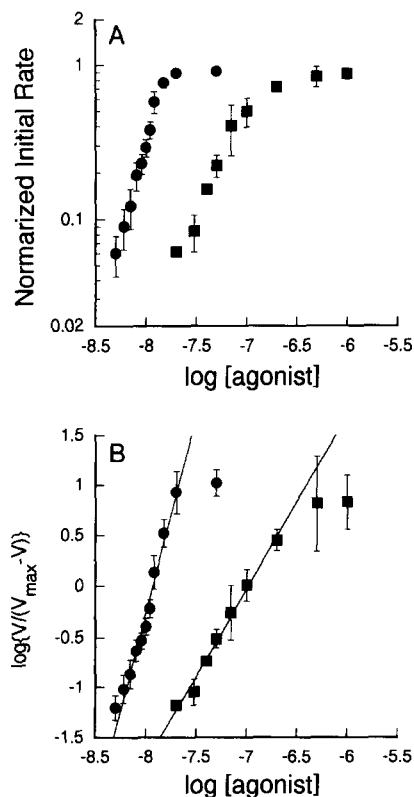


Fig. 4. Analysis of Ca^{2+} release induced by adenophostin (●) and IP_3 (■). (A) Normalized initial rates of Ca^{2+} release were plotted as a function of the concentration of adenophostin (●) and IP_3 (■). (B) Hill plot of Ca^{2+} release by adenophostin (●) and IP_3 (■) (values are mean \pm S.D., $n = 3-4$).

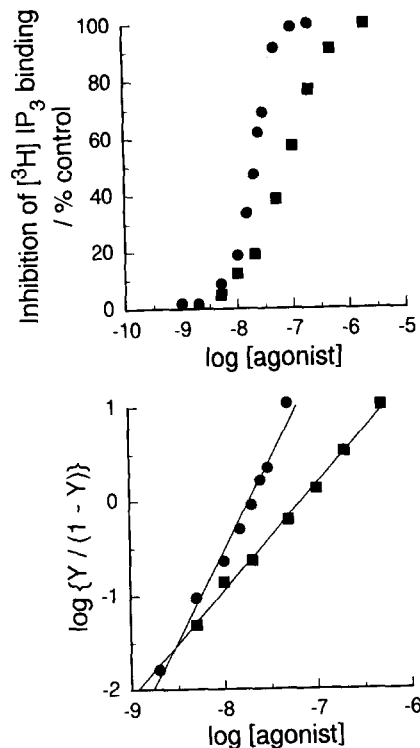


Fig. 5. Inhibition of [^3H]IP $_3$ binding to the purified IP $_3$ R1 by adenophostin (●) and IP $_3$ (■). The [^3H]IP $_3$ binding assay was carried out as described in section 2. (A) Displacement curves of [^3H]IP $_3$ binding in the presence of adenophostin (●) and IP $_3$ (■). (B) Hill plot of inhibition of [^3H]IP $_3$ binding ($Y/\%$ control) by adenophostin (●) and IP $_3$ (■). Measurements were duplicated.

$$K_i = (\text{IC}_{50} / (1 + C/K_d)) \quad (2)$$

where C represents a total concentration of [^3H]IP $_3$ ($C = 9.6$ nM) and K_d is dissociation constant of [^3H]IP $_3$ binding ($K_d = 11$ nM).

The affinities of adenophostin and IP $_3$ to the purified IP $_3$ R1 were well correlated to their Ca^{2+} releasing activities. Hill coefficients of the displacement curves of [^3H]IP $_3$ binding in the presence of adenophostin and IP $_3$ were 1.9 and 1.1, respectively (Fig. 5B), indicating that in terms of binding to IP $_3$ R1 adenophostin exhibited a positive cooperativity, whereas IP $_3$ did not. These results demonstrated that the difference in the cooperativity of ligand-binding may result in the difference in the cooperativity of Ca^{2+} releasing between both agonists.

3.4. Analysis of biphasic and quantal natures of adenophostin-induced Ca^{2+} release

To analyze the kinetic features of adenophostin-induced Ca^{2+} release in detail, we attempted to curve fit the profiles. All profiles of Ca^{2+} release consisted of the sum of two single exponentials as IP $_3$ did. The rate constants of the fast and slow components differed by a factor of about 10 (Fig. 6A) similar to those of IP $_3$ -induced Ca^{2+} release (Fig. 6B). Both the fast and slow rate constants were dependent on the concentrations of adenophostin and IP $_3$. The amplitudes of both states (A_{fast} and A_{slow}) derived from the curve fitting were plotted as a function of the concentrations of adenophostin and IP $_3$ (Fig. 6C and D). The amplitudes of the fast component increased as the concentration of adenophostin and IP $_3$ increased, whereas those of the slow components decreased. Considering these amplitudes with the amounts of total released Ca^{2+} , the amounts of released Ca^{2+} by the fast and slow phases were then calculated. The amounts of released Ca^{2+} by the fast and slow components

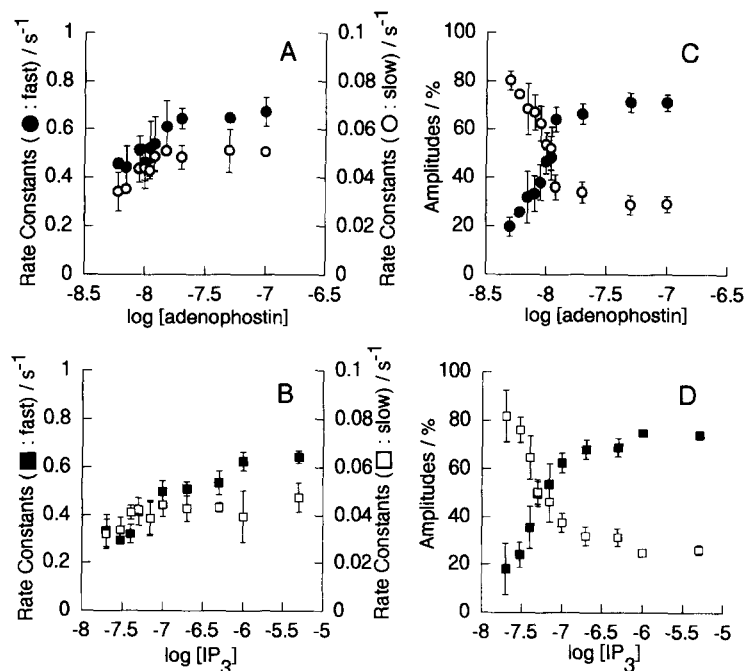


Fig. 6. Biexponential analysis of adenophostin- and IP $_3$ -induced Ca^{2+} release: Adenophostin dependence of the rate constants (A) and the amplitudes (C). IP $_3$ dependence of the rate constants (B) and the amplitudes (D). (A and C) The fast (●) and the slow (○) rate constants and amplitudes were plotted as a function of the concentration of adenophostin. (B and D) The fast (■) and slow (□) rate constants and amplitudes were plotted as a function of the concentration of IP $_3$ (values are mean \pm S.D., $n = 3-4$).

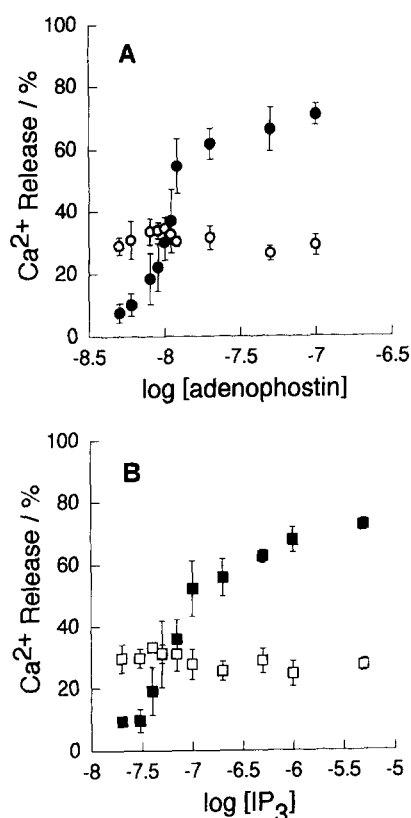


Fig. 7. The amounts of released Ca^{2+} by the fast and slow components of adenophostin-induced Ca^{2+} release (\bullet = fast; and \circ = slow) and IP_3 -induced Ca^{2+} release (\blacksquare = fast; and \square = slow). The amounts of total released Ca^{2+} (Fig. 3) and the amplitude of the two components of adenophostin-induced Ca^{2+} release (Fig. 6C) and IP_3 -induced Ca^{2+} release (Fig. 6D) allowed us to calculate the amounts of released Ca^{2+} by the fast (the closed symbols) and slow (the open symbols) components (values are mean \pm S.D., $n = 3$ –4).

relative to that of 100 nM adenophostin and 5 μM IP_3 were plotted as the function of the concentrations of adenophostin and IP_3 (Fig. 7A and B). The amounts of released Ca^{2+} by the fast component increased as a function of the concentrations of adenophostin and IP_3 , whereas the amounts of the slow component were almost constant, i.e. already saturated, over the concentrations of adenophostin and IP_3 examined. These results suggest that the fast component is kinetically the state of low affinity for both adenophostin and IP_3 and high permeability of Ca^{2+} , but the slow component is of high affinity and low permeability. Since the fast phase of Ca^{2+} release increases with increasing IP_3 concentrations and the slow phase remains constant, our data demonstrates that the fast phase is not only the determinant of the amount of Ca^{2+} release but also responsible for the quantal Ca^{2+} release. In the $[^3\text{H}]\text{IP}_3$ binding experiments using IP_3 , we detected single state of $\text{IP}_3\text{R1}$, although two states were observed in Ca^{2+} releasing experiments. The difference of numbers of the state of $\text{IP}_3\text{R1}$ may be due to the difference in experimental conditions, i.e. pH, temperature and buffer compositions.

Recently, heterogeneity of IP_3R densities in pools, which had equal sensitivity to IP_3 , was reported to be responsible for biphasic Ca^{2+} release [18]. We wish to discuss such possibility. If this is the reason for biphasic nature of IICR, the amplitudes of the fast and slow components in the curve fitting should be

independent to the IP_3 concentrations, and the ratio of the amounts of released Ca^{2+} by the fast and slow components must be constant. Because in such an assumption, the amplitudes and the ratio of the amounts of released Ca^{2+} should reflect the distribution of such heterogeneity, i.e. the amplitudes and the amounts of the released Ca^{2+} by the fast and slow phases reflect numbers of IP_3 -sensitive Ca^{2+} pools with high and low density of IP_3R , respectively. However, in our experiments, the amplitudes of the fast and slow components, and the ratio of the total released Ca^{2+} were dependent on IP_3 concentrations, indicating that the biphasic nature of Ca^{2+} release was not due to such heterogeneity of receptor density. A possibility of heterogeneity in the size of individual Ca^{2+} pools was also excluded by the same reasons and by the direct observation using electron microscopy. The average diameter of the liposome was 170 ± 50 nm ($n = 300$) and the distribution of the size was represented in single peak (data not shown).

Here, we have demonstrated that adenophostin, a novel agonist of the IP_3R , is capable of producing the quantal response of Ca^{2+} release as IP_3 did, but exhibited different positive cooperativity in ligand-binding steps and high positive cooperativity in Ca^{2+} release from those of IP_3 . The present study has also demonstrated that the purified $\text{IP}_3\text{R1}$ has two states with different affinity for both adenophostin and IP_3 , i.e. a low affinity and high affinity state. This could arise from alternative splicing leading to the production of variants of $\text{IP}_3\text{R1}$. Alternatively, there may be two different states of a single IP_3R due to ligand-dependent inactivation or interconversion.

Acknowledgments: We wish to thank Drs. Michio Niinobe and Shinji Nakade for their help in purification of IP_3R and fruitful discussions, Dr. Lee G. Sayers for critical reading of the manuscript. This work was supported by grants of the Japanese Ministry of Education, Science and Culture and the Human Frontier Science Program.

References

- [1] Berridge, M.J. (1993) *Nature* 361, 315.
- [2] Furuichi, T., Yoshikawa, S., Miyawaki, A., Wada, K., Maeda, N. and Mikoshiba, K. (1989) *Nature* 342, 32.
- [3] Sudhof, T.C., Newton, C.L., Archer III, B.T., Ushkaryov, Y.A. and Mignery, G.A. (1991) *EMBO J.* 10, 3199.
- [4] Blondel, O., Takeda, J., Janssen, H., Seino, S. and Bell, G.I. (1993) *J. Biol. Chem.* 268, 11356.
- [5] Furuichi, T., Kohda, K., Miyawaki, A. and Mikoshiba, K. (1994) *Curr. Opin. Neurobiol.* 4, 294.
- [6] Sugiyama, T., Yamamoto-Hino, M., Miyawaki, A., Furuichi, T., Mikoshiba, K. and Hasegawa, M. (1994) *FEBS Lett.* 349, 191.
- [7] Takahashi, M., Tanzawa, K. and Takahashi, S. (1994) *J. Biol. Chem.* 269, 369.
- [8] Takahashi, M., Kagasaki, T., Hosoya, T. and Takahashi, S. (1993) *J. Antibiotics* 46, 1643.
- [9] Nakade, S., Rhee, S.K., Hamanaka, H. and Mikoshiba, K. (1994) *J. Biol. Chem.* 269, 6735.
- [10] Maeda, N., Niinobe, M. and Mikoshiba, K. (1990) *EMBO J.* 9, 61.
- [11] Iino, M. (1990) *J. Gen. Physiol.* 95, 1103.
- [12] Iino, M. and Endo, M. (1992) *Nature* 360, 76.
- [13] Finch, E.A., Turner, T.J. and Goldin, S.M. (1991) *Science* 252, 443.
- [14] Watras, J., Bezprozvanny, I. and Ehrlich, B.E. (1991) *J. Neurosci.* 11, 3239.
- [15] Champeil, P., Combettes, L., Berthon, B., Doucet, E., Orlowski, S. and Claret, M. (1989) *J. Biol. Chem.* 264, 17665.
- [16] Somlyo, A.V., Horiuti, K., Trentham, D.R., Kitazawa, T. and Somlyo, A.P. (1992) *J. Biol. Chem.* 267, 22316.
- [17] Meyer, T., Wensel, T. and Stryer, L. (1990) *Biochemistry* 29, 32.
- [18] Hirose, K. and Iino, M. (1994) *Nature* 372, 791.